

Ancestry-agnostic estimation of DNA sample contamination from sequence reads.

Fan Zhang^{1,2} (fanzhang@umich.edu)

Matthew Flickinger^{1,3} (mflick@umich.edu)

InPSYght Psychiatric Genetics Consortium

Gonçalo R. Abecasis^{1,3} (goncalo@umich.edu)

Michael Boehnke^{1,3} (boehnke@umich.edu)

Hyun Min Kang^{1,3*} (hmkang@umich.edu)

1. Center for Statistical Genetics, University of Michigan, Ann Arbor, MI
2. Department of Computational Medicine and Bioinformatics, University of Michigan Medical School, Ann Arbor, MI
3. Department of Biostatistics, School of Public Health, University of Michigan, Ann Arbor, MI

*Correspondence to:

hmkang@umich.edu

1 Abstract

2 Detecting and estimating DNA sample contamination are important steps to ensure high quality
3 genotype calls and reliable downstream analysis. Existing methods rely on population allele
4 frequency information for accurate estimation of contamination rates. Correctly specifying
5 population allele frequencies for each individual in early stage of sequence analysis is impractical or
6 even impossible for large-scale sequencing centers that simultaneously process samples from
7 multiple studies across diverse populations. On the other hand, incorrectly specified allele
8 frequencies may result in substantial bias in estimated contamination rates. For example, we
9 observed that existing methods often fail to identify 10% contaminated samples at a typical 3%
10 contamination exclusion threshold when genetic ancestry is misspecified. Such an incomplete
11 screening of contaminated samples substantially inflates the estimated rate of genotyping errors
12 even in deeply sequenced genomes and exomes.

13 We propose a robust statistical method that accurately estimates DNA contamination and is
14 agnostic to genetic ancestry of the intended or contaminating sample. Our method integrates the
15 estimation of genetic ancestry and DNA contamination in a unified likelihood framework by
16 leveraging individual-specific allele-frequencies projected from reference genotypes onto principal
17 component coordinates. We demonstrate this method robustly and accurately estimates
18 contamination rates across different populations and contamination rates. We further demonstrate
19 that in the presence contamination, quantitative estimates of genetic ancestry (e.g. principal
20 component coordinates) can be substantially biased if contamination is ignored, and that our
21 proposed method corrects for this bias. Our method is publicly available at
22 <http://github.com/Griffan/verifyBamID>

23 Introduction

24 Sample contamination is a common problem in DNA sequencing studies. Contamination may
25 occur during sample shipment (due to spillage across wells, pipetting errors, insufficient dry ice),
26 library preparation (due to gel cut-through in fragment size selection or unexpected switch
27 between barcoded adaptors *in-vitro*), *in-silico* demultiplexing from a sequenced lane into barcoded
28 samples, or on many other unexpected occasions. Even modest levels of contamination (e.g. 2-5%)
29 within a species substantially increase genotyping error, even for deeply sequenced genomes¹.
30 Accurate estimation of DNA contamination rates allow us to identify and exclude contaminated
31 samples from downstream analysis, and genotypes of moderately contaminated samples (e.g.
32 <10%) can be improved by accounting for contamination in genotype calling¹.

33 Previously we developed methods and a software tool, *verifyBamID*², to estimate DNA
34 contamination from sequence reads given known population allele frequencies of common
35 variants. Many investigators and most major sequencing centers use *verifyBamID* as a part of their
36 standard sequence processing pipeline. However, we have shown that *verifyBamID* can
37 underestimate DNA contamination rates if the assumed population allele frequencies are
38 inaccurate². Such an underestimation can be avoided if correct population allele frequencies are
39 provided in an ideal circumstances. However, in early stage of sequence analysis, performing a
40 tailored customization of quality control (QC) steps for each sequenced genome based on their
41 ancestry is not always feasible or or sometimes impossible. Such a tailored customization requires
42 planned coordination between sequencing centers and study investigators prior to sequencing to
43 share the self-reported ancestry (which is not always accurate) or estimated ancestry from external

44 genotypes (which is not always available). Modifying the QC pipeline to accommodate study-
45 specific or sample-specific parameters may not be a possible option for large sequencing centers.
46 Even if such a tailored customization of QC pipeline is possible, preparing per-sample ancestry prior
47 to QC may delay time-sensitive issues in the sequencing procedure. If contamination rates can be
48 accurately estimated without having to know the ancestry or allele frequencies a priori this will
49 simplify the sequence analysis pipeline and expedite the QC.

50 Here we describe a novel method to robustly detect and estimate DNA contamination by
51 modelling the probability of observed sequence reads as a function of “individual-specific allele
52 frequencies” that account for genetic ancestry of a sample. Instead of assuming that the population
53 allele frequencies are known, we represent individual-specific allele frequencies as a function of
54 genetic ancestry using principal component coordinates and the reference genotypes from a
55 diverse population, e.g. Human Genome Diversity Project (HGDP)³ or 1000 Genomes⁴. We then
56 jointly estimate genetic ancestry and contamination rates of a sequenced individual based on a
57 mixture model, without requiring the assumption that population allele frequencies are known.

58 Our method enables accurate ancestry-agnostic estimation of contamination through a unified
59 likelihood framework that incorporates genetic ancestry and contamination together. We show that
60 our method provides (1) comparable or more accurate estimates of genetic ancestry than existing
61 methods such as *TRACE/LASER*^{5,6} even in the absence of contamination and (2) reduced bias in
62 contamination rate estimates compared to our previous method requiring known population allele
63 frequencies using *in silico* contaminated datasets and sequenced genomes from the InPSYght
64 psychiatric genetics sequencing study.

65 Material and Methods

66 We aim to jointly estimate sample contamination rates and genetic ancestry from sequence
67 reads without specifying population allele frequencies. First, we describe our previous mixture
68 model to estimate contamination rates assuming population allele frequencies are known. Second,
69 we introduce a model for sequence reads using population allele frequencies as a function of
70 genetic ancestry represented in principal component coordinates. Third, we extend the model to
71 enable joint estimation of contamination rates and genetic ancestry. Fourth, we evaluate our
72 methods using *in silico* contaminated samples and whole genome sequence data from the InPSYght
73 study.

74 Likelihood-based mixture model for DNA sequence contamination

75 In our previous contamination detection methods², we assumed that the DNA sequence reads
76 from an intended sample are contaminated by sequence reads from at most one contaminating
77 sample from the same population, and that the population allele frequencies of all analyzed genetic
78 variants are known. For each bi-allelic variant i ($1 \leq i \leq m$), let $b_{ij} \in \{R, A, O\}$ ($1 \leq j \leq D_i$) be the
79 observed base call representing the reference allele (R), alternate allele (A), or other allele (O) for
80 the j -th read that overlaps the variant; D_i is the observed sequence depth at variant i . Let $e_{ij} \in$
81 $\{0,1\}$ be a random variable indicating whether a sequencing error did (1) or did not (0) occur for
82 observed base b_{ij} ; we assume e_{ij} follows a Bernoulli distribution with success probability $10^{-\frac{Q_{ij}}{10}}$
83 where Q_{ij} is a phred-scale base quality score of b_{ij} . In the absence of contamination, if the true
84 genotype $g_i \in \{0,1,2\}$ represents the count of alternate alleles of the sequenced sample, then

85 $\Pr(b_{ij}|g_i^s, e_{ij})$ can be easily represented as in Table 1, making the simplifying assumption of equally
86 likely errors across four possible nucleotides.

87 We assume that the observed sequence reads are a $(1 - \alpha) : \alpha$ mixture of intended and
88 contaminating reads given a contamination rate $0 \leq \alpha \leq 1$. Let g_i^1 and g_i^2 represent the true
89 genotypes of the intended and contaminating samples at variant i , respectively. Then the mixture
90 model likelihood of each observed base becomes

$$91 \quad \Pr(b_{ij}|g_i^1, g_i^2, e_{ij}; \alpha) = (1 - \alpha)\Pr(b_{ij}|g_i^1, e_{ij}) + \alpha\Pr(b_{ij}|g_i^2, e_{ij}) \quad (1)$$

92 Assuming a homogenous population with known population allele frequency f_i and Hardy-
93 Weinberg Equilibrium (HWE), $\Pr(g_i^2; f_i)$ follows a Binomial($2, f_i$) distribution. Under the
94 simplifying assumption of independent variants, the likelihood of the contamination rate becomes

$$95 \quad L(\alpha) = \prod_{i=1}^m \sum_{g_i^1} \sum_{g_i^2} \left\{ \prod_{j=1}^{D_i} \sum_{e_{ij}} \Pr(b_{ij}|g_i^1, g_i^2, e_{ij}; \alpha) \Pr(e_{ij}) \right\} \Pr(g_i^2; f_i) \Pr(g_i^1; f_i) \quad (2)$$

96 The maximum likelihood estimate (MLE) of contamination rate $\hat{\alpha}$ can be obtained using Brent's
97 algorithm⁷.

98 As we previously reported², this model assumes correctly specified population allele frequencies
99 f_i .

100 Likelihood-based estimation of genetic ancestry (in the absence of contamination)

101 We extend this model to incorporate genetic ancestry. The key idea of this extension is to use
102 the individual-specific allele frequency (ISAF)^{8,9} to model the likelihood of the sequence reads.
103 Several methods, including Spatial Ancestry Analysis (SPA)¹⁰ and logistic factor analysis (LFA)⁹,

104 previously proposed modelling allele frequency as a function of genetic ancestry via principal
105 component (PC) coordinates.

106 Let G be an $m \times n$ genotype matrix (where $g_{ij} = 0, 1,$ or 2 is the number of non-reference
107 alleles at variant i in individual j) of a genetically diverse reference panel of size n , such as 1000
108 Genomes or HGDP. We define ISAF f_i ($0 \leq f_i \leq 1$) for variant i as a weighted average of genotypes
109 from the reference panel ($f_i = \sum_{r=1}^n w_r G_{ir}$), where $0 \leq w_r \leq 1$ and $G_{ir} \in \{0,1,2\}$ for individual r .
110 For a homogenous population, $w_r = \frac{1}{2n}$ results in a *pooled allele frequency* across all individuals in
111 the reference panel. If each individual can be categorically represented as a one of k mutually
112 exclusive subpopulations, the *population-specific allele frequency* for the subpopulation $s \in$
113 $\{1,2, \dots, k\}$ can be represented as $w_r = \frac{I(s_r=s)}{2n_s}$, where $s_r \in \{1,2, \dots, k\}$ represents the
114 subpopulation that individual r belongs to, and n_s represents the size of subpopulation s . More
115 generally, if individual's genetic ancestry is represented as continuous variables (such as PCs, SPAs,
116 or LFAs), the individual-specific allele frequency (ISAF) can be represented as a function of the
117 continuously represented genetic ancestry^{9,5}.

118 The estimated ISAF can be viewed as (one half times the) genotype dosages approximated from
119 a fixed number(= K) of factors, such as PCs, SPAs, or LFAs. In our method, we used a linear model to
120 estimate ISAF from PCs, similar to previous studies^{8,9}. Given the reference panel genotype matrix G ,
121 let $\frac{1}{2} \hat{G}$ be the *ISAF matrix* as a function of top K factors. ISAF matrix $\frac{1}{2} \hat{G}$ should well approximate
122 $\frac{1}{2} G$. For example, under a linear model, typical principal component analysis takes the singular
123 value decomposition (SVD) of the mean-centered genotype matrix $\bar{G} = G - 2\mu\mathbf{1}_n^T = UDV^T$, where
124 $\mu = \frac{1}{2n} G\mathbf{1}_n$ is the pooled allele frequencies and $\mathbf{1}_n$ is the column-vector of ones. Using the top K

125 eigenvalues and corresponding eigenvectors $U^{(K)}, D^{(K)}, V^{(K)}$ from the SVD, it is known that $\hat{G} =$
126 $\frac{1}{2} U^{(K)} D^{(K)} [V^{(K)}]^T + \boldsymbol{\mu} \mathbf{1}_n^T$ minimizes $\|G - \hat{G}\|_2 = \sum_{i,j} (G_{ij} - \hat{G}_{ij})^2$ among all possible rank K
127 matrices¹¹, making it a good proxy for the ISAF matrix.

128 For a new individual s with genetic ancestry represented as $\mathbf{x}_s \in \mathbb{R}^k$ in the PC (eigenvector)
129 space of the reference panel, the ISAF for i -th variant can be modelled as $f_i(\mathbf{x}_s) = \frac{1}{2} \mathbf{u}_i^{(K)} D^{(K)} \mathbf{x}_s^T +$
130 μ_i , where $\mathbf{u}_i^{(K)}$ is i -th row of $U^{(K)}$ and μ_i is the i -th element of $\boldsymbol{\mu}$. To avoid boundary condition, we
131 constrain $\frac{\varepsilon}{2n} \leq f_i(\mathbf{x}_s) \leq 1 - \frac{\varepsilon}{2n}$ for a fixed ε (we used $\varepsilon = 0.5$ in our experiments). Then the overall
132 likelihood of an individual's genetic ancestry \mathbf{x} is

$$133 \quad L(\mathbf{x}_s) = \prod_{i=1}^m \sum_{g_i} \left\{ \prod_{j=1}^{D_i} \sum_{e_{ij}} \Pr(b_{ij} | g_i, e_{ij}) \Pr(e_{ij}) \right\} \Pr(g_i; f_i(\mathbf{x}_s)) \quad (3)$$

134 where g_i represents the unobserved genotype of the sequenced sample at variant i . The maximum-
135 likelihood genetic ancestry coordinates can be estimated as $\hat{\mathbf{x}}_s = \operatorname{argmax}_{\mathbf{x}_s \in \mathbb{R}^k} L(\mathbf{x}_s)$ using the
136 Nelder-Mead¹² algorithm, starting with PC coordinates of a randomly selected individual from the
137 reference panel. In our experiments, we always obtained consistent estimates of $\hat{\mathbf{x}}_s$ regardless of
138 start values.

139 Joint estimation of genetic ancestry and DNA contamination

140 Because our goal is to obtain unbiased estimates of the DNA contamination rate α agonistic to
141 genetic ancestry, we propose to jointly estimate α and ancestry by combining the models described
142 in the previous sections. Let $\mathbf{x}_1, \mathbf{x}_2 \in \mathbb{R}^k$ be the genetic ancestries of the intended and
143 contaminating samples. Then the likelihood under the combined model is

$$L(\alpha, \mathbf{x}_1, \mathbf{x}_2) = \prod_{i=1}^m \sum_{g_i^1} \sum_{g_i^2} \left\{ \prod_{j=1}^{D_i} \sum_{e_{ij}} \Pr(b_{ij} | g_i^1, g_i^2, e_{ij}; \alpha) \Pr(e_{ij}) \right\} \Pr(g_i^1; f_i(\mathbf{x}_1)) \Pr(g_i^2; f_i(\mathbf{x}_2))$$

145 When the contamination rate $\alpha \approx 0$, the parameters corresponding to \mathbf{x}_2 do not contribute
146 (much) to the likelihood and the estimates of \mathbf{x}_2 may be unstable. To address this problem, we
147 initially assume that the intended and contaminating samples are from the same population $\mathbf{x}_1 =$
148 \mathbf{x}_2 ('equal-ancestry' model) and then repeat the analysis allowing for $\mathbf{x}_1 \neq \mathbf{x}_2$ ('unequal-ancestry'
149 model). The dimension of parameter space for the unequal-ancestry model is $2k + 1$. We choose
150 final parameter estimates between the two models based on Akaike Information Criterion (AIC)¹³.

151 Evaluation on *in-silico* contaminated data based on 1000 Genomes project samples

152 We constructed *in-silico* contaminated DNA sequence reads using aligned low-coverage whole
153 genome sequence reads from the 1000 Genomes phase 3 project⁴. We filtered out unmapped and
154 mark-duplicated reads and then randomly sampled aligned sequence reads proportional to the
155 intended contamination rates $\alpha \in \{0.01, 0.02, 0.05, 0.1, 0.2\}$. To match the mixing proportion of
156 sequence reads originated from intended and contaminating to be $(1 - \alpha) : \alpha$, each read was
157 sampled with probability $(1 - \alpha)$ and $\frac{B_1}{B_2} \alpha$ from each sample, where B_1 and B_2 are number of
158 aligned bases from unique reads from intended and contaminating samples. We selected four
159 populations, CHS (Han Chinese South), GBR (British in England and Scotland), MXL (Mexican
160 Ancestry from Los Angeles USA), YRI (Yoruba in Ibadan, Nigeria), and arbitrarily selected 10 pairs of
161 individuals with similar sequencing depths within the same population and across populations. To
162 estimate genetic ancestry and/or contamination rate for these *in-silico* contaminated sequence
163 reads, we used a reference panel of 938 HGDP³ individuals across 1,000, 10,000 and 100,000

164 randomly chosen SNPs (pooled MAF > 0.5%), avoiding variants masked by the 1000 Genomes
165 Project⁴ (See Web Resource). When we compared estimated genetic ancestry with *LASER*, we used
166 the same set of selected SNPs and sequence reads as input. For *TRACE*, we used genotypes from the
167 phase 3 release (for 1000 Genomes) or an interim callset from the *GotCloud* software tool¹⁴ (for
168 InPSYght, see next section for details) on the same SNP set.

169 Experiment with real sequence data from the InPSYght study

170 Next, we applied our method to 500 deeply sequenced (mean depth 32x) genomes from the
171 first two batches of the InPSYght study. For each sample, we evaluated the results from the six
172 models: (1) the original *verifyBamID* using pooled allele frequencies; the original *verifyBamID* using
173 (2) African, (3) East Asian, and (4) European allele frequencies; (5) the new *verifyBamID2* under the
174 equal-ancestry model; and (6) *verifyBamID2* under the unequal-ancestry model. To calculate
175 pooled, population-specific, and individual-specific allele frequencies, we used the 1000 Genomes
176 phase 3 reference panel (n=2,504), randomly selecting 100,000 SNPs among the sites also
177 polymorphic in Illumina Human Omni 2.5 array, with the same filtering criteria (MAF > 5% and 1000
178 Genomes mask) as above.

179

180 Results

181 We assessed our new methods in the following steps. First, in the absence of contamination, we
182 demonstrate that our estimation of genetic ancestry provides comparably accurate estimates of
183 genetic ancestry as other state-of-art methods. Second, in the presence of contamination, we
184 demonstrate that joint estimation of genetic ancestry and contamination substantially improves the
185 estimation accuracy of both parameters. Third, using *in-silico* contaminated samples, we
186 demonstrate that our methods robustly provide more accurate estimates than previous methods
187 across various combinations of genetic ancestries and contamination rates. Fourth, from the
188 analysis of deeply sequenced genomes in the InPSYght study, we demonstrate that our new
189 methods deliver more accurate contamination estimates than the previous methods.

190

191 [New model-based methods accurately estimate genetic ancestry.](#)

192 In the absence of contamination, widely used methods such as *LASER* and *TRACE* are known to
193 estimate genetic ancestry accurately. Because we propose using a new model-based approach to
194 estimate the genetic ancestry (jointly with contamination rates), we first compared the accuracy of
195 our new method, in the absence of contamination, with *LASER* and *TRACE*. We randomly chose 500
196 ethnically diverse samples from the 1000 Genomes Project low-coverage (4X) genomes, and 500
197 African American samples from the deeply sequenced (32x) genomes from the InPSYght project.
198 We estimated their genetic ancestries using 100,000 SNPs from the HGDP reference panel (see
199 Methods for details) and compared their genetic ancestry estimates obtained by *LASER* (using the
200 same sequence data), and *TRACE* (using the hard-call genotypes). As illustrated in Figure 1A, 1C, 1E,

201 the estimated PC coordinates of the 1000 Genomes individuals are located close to their
202 corresponding HGDP populations across all three methods. Compared to *TRACE* and *LASER*, we
203 observed that the estimated genetic coordinates from *verifyBamID2* were the closest to the
204 centroid of corresponding HGDP population (Table 2) in 4 of the 5 populations (all except TSI).
205 These results suggest that our method provides estimates at least as precise compared to those for
206 other state-of-the-art methods.

207 [Genetic ancestry estimates may be confounded by DNA contamination.](#)

208 Next, we constructed *in-silico* contaminated sequenced data from the 1000 Genomes Project
209 and estimated contamination parameters and genetic ancestries jointly. We observed that when
210 sequences are contaminated between different continental populations, the genetic ancestry esti-
211 mates in PC coordinates drift towards the contaminating population when contamination is ignored
212 (Figure 2A) or when assuming that intended and contaminating samples originated from the same
213 population (Figure 2B). As the contamination rate increases, drift increases.

214 However, when we accounted for possible differences in genetic ancestries between the two
215 intended and contaminating samples using our new methods, PC coordinates remained similar to
216 those for uncontaminated samples (Figure 2E), and contaminated samples constructed from indi-
217 viduals that belong to the same population (Figure 2B, 2D, 2F).

218 [Robust, accurate, ancestry-agnostic estimation of DNA contamination.](#)

219 Next, we evaluated the effect of genetic ancestry misspecification in estimating DNA
220 contamination rates. We constructed contaminated samples between various combinations of

221 populations, and compared the accuracy of estimated contamination rates using both the original
222 methods which assume known allele frequencies and the new methods which estimate
223 contamination rate and genetic ancestry jointly.

224 When contamination happens within the same population, running original methods with
225 correct continental population allele frequencies specified provided accurate contamination
226 estimates (Figure 3A, 3E, 3I). However, using pooled allele frequencies, which would be a default
227 option when it is infeasible to specify population information *a priori* before sequencing,
228 consistently underestimated contamination rates. Bias was particularly large when intended individ-
229 uals were of African ancestry.

230 Specifying incorrect population allele frequencies results in even larger contamination
231 estimation bias. For example, using African allele frequencies on East Asian samples resulted in an
232 average estimate of 2.9% contamination for samples with contamination 10% (Table S1), implying
233 that a large fraction of 10% contaminated samples within East Asian ancestry would not have been
234 flagged for contamination-based exclusion at the contamination-exclusion threshold of 1-3% used
235 by many studies e.g. the Trans-Omics Precision Medicine (TOPMed) study¹⁵.

236 Our results consistently demonstrated that the ancestry-agnostic method provides as accurate
237 estimates as the original methods specified with correct population labels (Figure 3A, 3E, 3I, Table
238 S1), and the estimates are substantially better than those from pooled allele frequencies or
239 incorrectly specified allele frequencies.

240 When the intended and contaminating populations are different, we observed that
241 contamination is sometimes overestimated due to increased fraction of heterozygous genotypes

242 than expected by a given contamination rate under single population model. Our method based on
243 unequal-ancestry model outperforms all the other methods in terms of overall bias and Mean
244 Squared Error(MSE) (Figure 3, Table S4), correcting for both upward and downward biases in
245 various ancestry combinations. For example, the relative deviation of estimated to intended
246 contamination rate (i.e. $|\hat{\alpha}/\alpha - 1|$) is reduced by 80% (73-88%) compared to the original
247 *verifyBamID* with various population allele frequencies, suggesting reduced bias. MSE is also
248 reduced by 92% (86-97%). This robustness reflects the ability to incorporate differences in
249 population allele frequencies between intended and contaminating individuals (Figure 3B, 3C, 3D,
250 3F, 3G, 3H, Table S1).

251 We also examined the accuracy of our methods for admixed populations by performing a similar
252 experiment using the Mexican population (MXL) and obtained consistent results (Supplementary
253 Table S2).

254 [Results with deep whole genome sequence data from the InPSYght study.](#)

255 Next, we applied our methods to 500 African American samples from the InPSYght study (see
256 Methods). Consistent with the results from our *in silico* contamination studies, we observed that
257 the average contamination rate was 1.1-fold higher with newer method (0.36% for unequal-
258 ancestry, 0.37% for equal-ancestry) compared to the original method with pooled allele frequency
259 (0.33%) (Figure 4). The number of samples with estimated contamination rate >1% increased from
260 16 (original method with pooled allele frequency) to 21 (unequal-ancestry method) or 23 (unequal-
261 ancestry method), suggesting our new method more rigorously screens for contaminated samples.

262 All 500 deeply sequenced genomes in InPSYght study are reported to be African Americans, and
263 indeed the estimated PC coordinates for all 500 individuals under all three methods lie between
264 European and African samples. Compared to other methods to estimate genetic ancestry, our
265 estimates resulted in tighter clustering along the European-African segment than *LASER*, and
266 similarly tight clustering to *TRACE* (Figure 1B, 1D, 1F). For example, the correlation coefficient
267 between the PC1 and PC2 coordinates were 0.927 for *LASER*, 0.981 for *TRACE*, and 0.985 for
268 *verifyBamID2*, corroborating that *verifyBamID2* results in more precise estimate of African ancestry
269 along the European-African segment in PC coordinates.

270 [Impact of number of markers on accuracy, computational cost, and memory requirements.](#)

271 As we have shown previously², there are trade-offs between computation cost and accuracy of
272 contamination estimates. Using as many as 100,000 variants results in accurately estimated intended
273 contamination rate. For example, MSE of relative deviation (i.e. $|\hat{\alpha}/\alpha - 1|$) was 0.02, 0.01, 0.01 when
274 the intended contamination was 1%, 2%, and 5%, respectively. When we use 10,000 variants, the
275 MSEs modestly increased to 0.11, 0.04, and 0.01, respectively. When we use only 1,000 variants,
276 MSEs further increased to 0.69, 0.25, 0.11, suggesting that the estimates may not be precise for low
277 contamination rate when using only 1,000 variants. (Supplementary Table S3).

278 We also evaluated the computational cost and memory consumption of *verifyBamID2* on whole
279 genome sequence data with various coverages. For the BAM files from the 1000 Genomes whole
280 genome sequence data (4.3-5.1x coverage), the average wall-clock running time was 5.5 minutes with
281 a single thread and peak memory consumption was 505 MB when using 10,000 markers in a server
282 with Xeon 2.27GHz processor. When using 100,000 markers, the average wall-clock running time was

283 20.5 minutes with a single thread and 8.0 minutes with four threads, and peak memory consumption
284 was 528 MB.

285 For deep genome data from the InPSYght study (31x coverage) stored in CRAM format, the
286 average wall-clock time was 17.3 minutes and peak memory consumption was 514 MB when using
287 10,000 markers. For 100,000 markers the average wall-clock time was 155.6 minutes (single thread)
288 or 96 minutes (four threads) and peak memory consumption was 548 MB.

289 Discussion

290 Contamination detection is an essential step in the sequence analysis process that has important
291 effects on following downstream analyses. Early and accurate estimation of DNA contamination can
292 prevent wasted effort, time, and money by identifying the problems early on before too many
293 samples are sequenced using contamination-prone protocols. Our previous method enabled such a
294 timely contamination detection from sequence data and population allele frequencies at known
295 variant sites, without requiring independent SNP genotype data. Our new method maintains these
296 advantages, and in addition provide three more. First, because our joint analysis method is agnostic
297 to genetic ancestry, it eliminates sample-to-sample variation in the parameter settings for the
298 contamination checking procedure, simplifying the sequence analysis pipeline. Second, it provides
299 more robust contamination estimates against potentially misspecified population allele frequency of
300 the intended (or contaminating) samples when relying on the reported ancestry information. Third,
301 it provides accurate estimates of genetic ancestries for both intended and contaminating samples.
302 This enables additional sanity checking of the sequence data, such as determining whether a
303 sequenced sample matches its expected (participant-reported) ancestry. It also facilitates
304 incorporating ancestry information in the variant calling and downstream analysis, and allows us to
305 track the source of contamination more precisely when contamination occurs.

306 Our method can be used not only to detect and estimate contamination, but also to estimate
307 genetic ancestry from sequence data. Relatively few methods, such as *LASER*^{5,6} and *bammds*¹⁶, exist
308 for estimating genetic ancestry from sequence data while several methods have been developed for
309 array-based genotypes, such as *EIGENSOFT*¹⁷, *FRAPPE*¹⁸, *ADMIXTURE*¹⁹, and *TRACE*⁶. We have

310 demonstrated that our method provides ancestry estimates as or more accurate than *LASER*,
311 particularly when the sequenced samples are contaminated between different ancestries.

312 By jointly estimating genetic ancestry and contamination, we are able to accurately estimate
313 contamination without requiring ancestry information *a priori*. Since obtaining population allele
314 frequency information may be infeasible or even impossible at the time of sequencing, it is important
315 to highlight that our ancestry-agnostic approach provides more timely and accurate feedback to the
316 sequencing facilities. Our ancestry-agnostic approach also simplifies the sequence analysis pipeline,
317 because the same input arguments can be applied across all samples regardless of their genetic
318 ancestry

319 The key idea of using individual-specific allele frequencies (ISAF) to account for population
320 structure in genetic analysis has been suggested previously in the context of characterizing
321 population structure or identifying highly differentiated variants across populations^{8,9}. To the best
322 of our knowledge, our method describes the first likelihood-based model utilizing ISAF to represent high
323 throughput sequence reads under population structure and/or contamination. While previous
324 studies proposed logistic models as alternative to linear model^{8,9}, we used linear models (bounded
325 by minimum and maximum value) between allele frequencies and population structure represented
326 by Singular Value Decomposition (SVD) on the genotype matrix. We made this choice because the
327 logistic model is computationally more intensive, and the linear model is accurate for the common
328 variants we use, as demonstrated by the previous studies⁹.

329 Because we use Nelder-Mead optimization for maximum likelihood estimation, it is possible that
330 the estimates do not converge to the global maximum, especially when many principal components
331 are used. We observed that estimating the full unequal-ancestry model parameters sometimes does

332 fail to converge especially when there is little or no contamination, due to the limited identifiability
333 of the genetic ancestry of contaminating samples in this situation. Starting by estimating
334 contamination rate and shared genetic ancestry parameters using the equal-ancestry model, and
335 using those estimates as start values for the unequal-ancestry model to allow different ancestries
336 between the intended and contaminating samples dramatically improved convergence; in fact, the
337 method converged to consistent estimates across multiple starting points within 1,000 iterations in
338 all our benchmark cases, in both real and *in-silico* contaminated data. When the contamination rate
339 is extremely small (e.g. <0.1%), estimation of genetic ancestry of contaminating samples can still be
340 challenging. We allow unequal ancestries between intended and contaminating samples only when
341 the likelihood substantially improves beyond AIC threshold between equal ancestry and unequal
342 ancestry models. This procedure effectively removed all outlier estimates of genetic ancestries of
343 contaminating samples in our experiments.

344 There are other possible useful extensions to our joint contamination and estimation method.
345 We are extending these methods to detect and estimate contamination for RNA-seq and other
346 epigenomic sequence data. The same model has potential applications in other areas, such as cancer
347 single cell transcriptomics²⁰.

348 We expect that our new *verifyBamID2* software will facilitate more accurate, convenient, and
349 timely quality control of sequence genomes. Our software tool is publicly available at
350 <http://github.com/Griffan/verifyBamID>. Our GitHub repository provides reference files that can be
351 used as test input for our methods. These files contain key input files required for *verifyBamID2*,
352 including variant loadings, supporting various genome builds (GRCh37 and GRCh38), and various
353 numbers of variants.

354 **Web Resources**

355 1000 genomes project genome mask file:

356 (ftp://ftp.1000genomes.ebi.ac.uk/vol1/ftp/release/20130502/supporting/accessible_genome_mask
357 [s/StrictMask/](ftp://ftp.1000genomes.ebi.ac.uk/vol1/ftp/release/20130502/supporting/accessible_genome_mask))

358

359 **Acknowledgements**

360 This work was supported by NIH grants HG009976 (to M.F. and M.B.), HL137182 (to H.M.K. and F.Z),
361 HG007022 (to G.R.A), MH105653 (to M.B, InPSYght Consortium, and H.M.K.)

362

363 **References**

364 1. Flickinger, M., Jun, G., Abecasis, G.R., Boehnke, M., and Kang, H.M. (2015). Correcting for sample
365 contamination in genotype calling of DNA sequence data. *Am. J. Hum. Genet.* *97*, 284–290.

366 2. Jun, G., Flickinger, M., Hetrick, K.N., Romm, J.M., Doheny, K.F., Abecasis, R., Boehnke, M., and
367 Kang, H.M. (2012). Detecting and estimating contamination of human DNA samples in sequencing
368 and array-based genotype data. 839–848.

369 3. Cavalli-Sforza, L.L. (2005). The Human Genome Diversity Project: past, present and future. *Nat*
370 *Rev Genet* *6*, 333–340.

371 4. The 1000 Genomes Project Consortium (2015). A global reference for human genetic variation.
372 *Nature* *526*, 68–74.

- 373 5. Wang, C., Zhan, X., Bragg-Gresham, J., Kang, H.M., Stambolian, D., Chew, E.Y., Branham, K.E.,
374 Heckenlively, J., Fulton, R., Wilson, R.K., et al. (2014). Ancestry estimation and control of
375 population stratification for sequence-based association studies. *Nat. Genet.* *46*, 409–415.
- 376 6. Wang, C., Zhan, X., Liang, L., Abecasis, G.R., and Lin, X. (2015). Improved ancestry estimation for
377 both genotyping and sequencing data using projection procrustes analysis and genotype
378 Imputation. *Am. J. Hum. Genet.* *96*, 926–937.
- 379 7. Brent, R.P. (1974). Algorithms for minimization without derivatives. *IEEE Trans. Automat. Contr.*
- 380 8. Conomos, M.P., Reiner, A.P., Weir, B.S., and Thornton, T.A. (2016). Model-free estimation of
381 recent genetic relatedness. *Am. J. Hum. Genet.* *98*, 127–148.
- 382 9. Hao, W., Song, M., and Storey, J.D. (2015). Probabilistic models of genetic variation in structured
383 populations applied to global human studies. *Bioinformatics* *32*, 713–721.
- 384 10. Yang, W.W.-Y., Novembre, J., Eskin, E., and Halperin, E. (2012). A model-based approach for
385 analysis of spatial structure in genetic data. *Nat. Genet.* *44*, 725–731.
- 386 11. Pearson, K. (1901). LIII. *On lines and planes of closest fit to systems of points in space*. *Philos.*
387 *Mag. Ser. 6* 2, 559–572.
- 388 12. Nelder, J.A., and Mead, R. (1965). A simplex method for function minimization. *Comput. J.* *7*,
389 308–313.
- 390 13. Akaike, H. (1974). A new look at the statistical model identification. *IEEE Trans. Automat. Contr.*
- 391 14. Jun, G., Wing, M.K., Abecasis, G.R., and Kang, H.M. (2015). An efficient and scalable analysis
392 framework for variant extraction and refinement from population-scale DNA sequence data.

393 Genome Res. 25, 918–925.

394 15. Natarajan, P., Peloso, G.M., Zekavat, S.M., Montasser, M., Ganna, A., Chaffin, M., Khera, A. V.,
395 Zhou, W., Bloom, J.M., Engreitz, J.M., et al. (2018). Deep-coverage whole genome sequences and
396 blood lipids among 16,324 individuals. Nat. Commun.

397 16. Malaspinas, A.S., Tange, O., Moreno-Mayar, J.V., Rasmussen, M., DeGiorgio, M., Wang, Y.,
398 Valdiosera, C.E., Politis, G., Willerslev, E., and Nielsen, R. (2014). bammds: a tool for assessing the
399 ancestry of low-depth whole-genome data using multidimensional scaling (MDS). Bioinformatics
400 30, 2962–2964.

401 17. Price, A.L., Patterson, N.J., Plenge, R.M., Weinblatt, M.E., Shadick, N. a, and Reich, D. (2006).
402 Principal components analysis corrects for stratification in genome-wide association studies. Nat.
403 Genet. 38, 904–909.

404 18. Tang, H., Peng, J., Wang, P., and Risch, N.J. (2005). Estimation of individual admixture: Analytical
405 and study design considerations. Genet. Epidemiol. 28, 289–301.

406 19. Alexander, D.H., Novembre, J., and Lange, K. (2009). Fast model-based estimation of ancestry in
407 unrelated individuals. Genome Res. 19, 1655–1664.

408 20. Kang, H.M., Subramaniam, M., Targ, S., Nguyen, M., Maliskova, L., McCarthy, E., Wan, E., Wong,
409 S., Byrnes, L., Lanata, C.M., et al. (2018). Multiplexed droplet single-cell RNA-sequencing using
410 natural genetic variation. Nat. Biotechnol.

411

412

413

Table 1. Conditional probability $P(b_{ij} | g_i, e_{ij})$ of read b_{ij} given true genotype g_i and the variable representing the event of base calling error e_{ij} , as described in (Jun et al 2012²)

True Genotype g_i	Base Calling Error Event e_{ij}	$\Pr(b_{ij} = R)$	$\Pr(b_{ij} = A)$	$\Pr(b_{ij} = O)^b$
$g_i = RR^a$	$e_{ij} = 0$	1	0	0
	$e_{ij} = 1$	0	1/3	2/3
$g_i = RA^a$	$e_{ij} = 0$	1/2	1/2	0
	$e_{ij} = 1$	1/6	1/6	2/3
$g_i = AA^a$	$e_{ij} = 0$	0	1	0
	$e_{ij} = 1$	1/3	0	2/3

^a RR, RA, AA: homozygous reference, heterozygous, and homozygous non-reference genotypes

^b O: alleles other than R or A; assumes four possible alleles (bases)

414

Table 2. Distance between estimated PCA coordinates of HGDP and 1000G populations*

Population Label		<i>TRACE</i>	<i>LASER</i>	<i>verifyBamID2</i>
1000G	HGDP			
CHB	Han-NChina	1.68	2.61	0.40
CHS	Han	1.70	1.24	1.18
TSI	Tuscan	1.52	2.16	1.81
YRI	Yoruba	2.32	1.73	0.42
JPT	Japanese	1.54	1.03	1.22

*Distances were measured between the mean PCA coordinates across the population in HGDP (estimated from the array data of Wang et al.⁶) and the mean PCA coordinates estimated from 1000 Genomes low coverage sequence data of the corresponding population, projected onto the same PCA coordinates using *TRACE*, *LASER*, or *verifyBamID2* (assuming no contamination). Bold face represents the smallest distance among the three methods for each population.

Table 3. Average contamination estimates for 5% contaminated samples (size n=10).

Sample Population		Original Model (Fixed Allele Frequencies)				Equal-Ancestry Model	Unequal-Ancestry Model
Intended	Contaminating	European	East Asian	African	Pooled		
GBR	GBR	4.73%	3.19%	2.67%	3.76%	4.63%	4.63%
CHS	CHS	1.90%	4.73%	1.25%	2.38%	4.73%	4.76%
YRI	YRI	1.78%	1.58%	4.44%	2.45%	4.40%	4.40%
CHS	YRI	3.33%	6.91%	2.27%	4.10%	6.71%	4.81%
YRI	CHS	2.79%	2.55%	6.29%	3.76%	5.99%	4.67%
GBR	YRI	6.13%	4.16%	3.60%	5.04%	5.90%	4.83%
YRI	GBR	2.81%	2.57%	6.38%	3.80%	6.01%	4.63%
CHS	GBR	2.87%	6.33%	1.98%	3.55%	6.13%	4.83%
GBR	CHS	5.32%	3.78%	3.05%	4.32%	5.16%	4.67%

416 Average contamination estimates of *in-silico* contaminated samples when the true contamination
417 rate is 5%. Each mixing configuration (e.g. GBR+CHS) contains 10 samples that are constructed with
418 95% reads coming from the intended sample and 5% reads from the contaminating sample. The
419 estimated contamination rates are obtained using the original version *verifyBamID* by specifying
420 prior allele frequencies as European, East Asian, African, and Pooled, respectively. Bold represents
421 the closest estimate to the true value of 5%.

422 Figure Legends

423

424 Figure 1.

425 Evaluation of estimated genetic ancestry coordinates, in the absence of contamination, between
426 *TRACE*, *LASER*, and *verifyBamID2* on samples from the 1000 Genomes low coverage genome (n=500,
427 diverse ancestry) sequence data (A,C,E) and from the InPSYght deep genome (n=500, African
428 Americans) sequence data (B,D,F). Panels A and B show results from *TRACE*, C and D from *LASER*, and
429 E and F from *verifyBamID2* (assuming no contamination). Each point represents a sample and each
430 color represents a population ancestry with the exception that grey point represents PCA coordinates
431 of reference (HGDP) samples.

432

433 Figure 2.

434 Impact of DNA sample contamination on the estimation of genetic ancestry. Each point represents a
435 sample. Each grey point represents reference (HGDP) sample and its PCA coordinates, similar to
436 Figure 1. Each colored point represents *in-silico* contaminated samples across various
437 contamination rates and populations. In panels A, C, and E, European (GBR) and East Asian (CHS)
438 samples are contaminated with African (YRI) samples at different contamination rates (i.e.
439 between-ancestry contamination). In panel B, D, and F, European (GBR) and East Asian (CHS)
440 samples are contamination with another sample in the same population (i.e. within-ancestry
441 contamination). Different colors represent different contamination rates ranging from 1% to 20%.
442 Upper panels (A, B) show *verifyBamID2* estimates without modelling contamination, middle panels
443 (C, D) *verifyBamID2* estimates under the assumption that intended and contaminating populations
444 are identical (i.e. equal-ancestry model), lower panels (E, F) *verifyBamID2* estimates under the
445 assumption that intended and contaminating populations can be different (i.e. unequal-ancestry
446 model).

447

448 Figure 3.

449 Comparison of different models to estimate contamination rates. Horizontal (x) axis shows intended
450 contamination rate, vertical (y) axis shows the ratio of estimated to intended contamination rates.
451 Each color represents different models to estimate contamination rates. EUR_AF, EAS_AF, and
452 AFR_AF represent original *verifyBamID* using European, East Asian, and African allele frequencies
453 across the continental population using the 1000 Genomes data. Pooled_AF represents the original
454 *verifyBamID* using aggregated allele frequencies across all 2,504 individuals in the 1000 Genomes
455 Project. Equal_Ancestry represents the *verifyBamID2* assuming that intended and contaminating
456 samples belong to the same population. Unequal_Ancestry represents *verifyBamID2* allowing
457 different genetic ancestry between intended and contaminating sample (recommended setting).

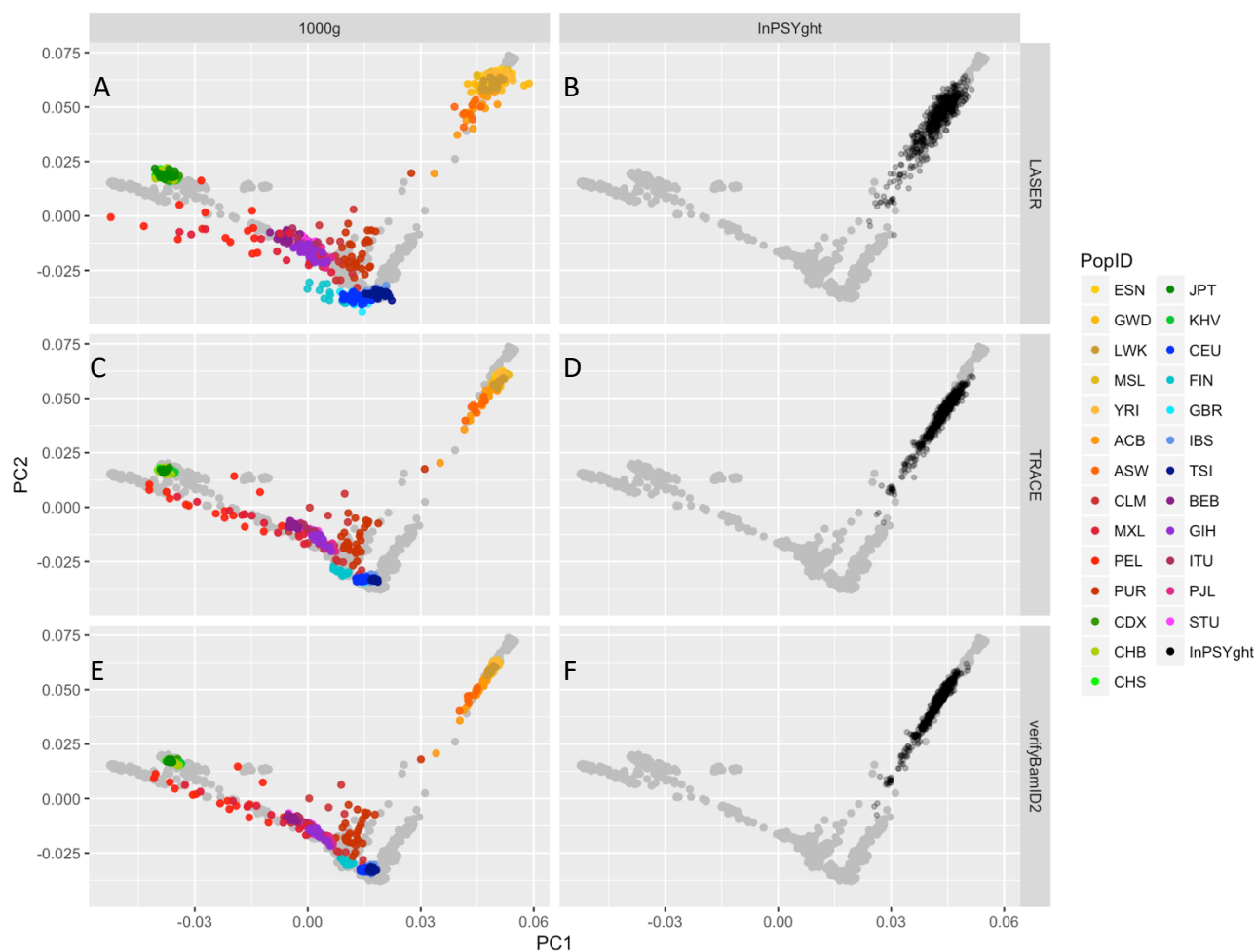
458 Each panel represents different combinations of intended (row) and contaminating (column)
459 populations, in the order of GBR, CHS, and YRI.

460

461 Figure 4

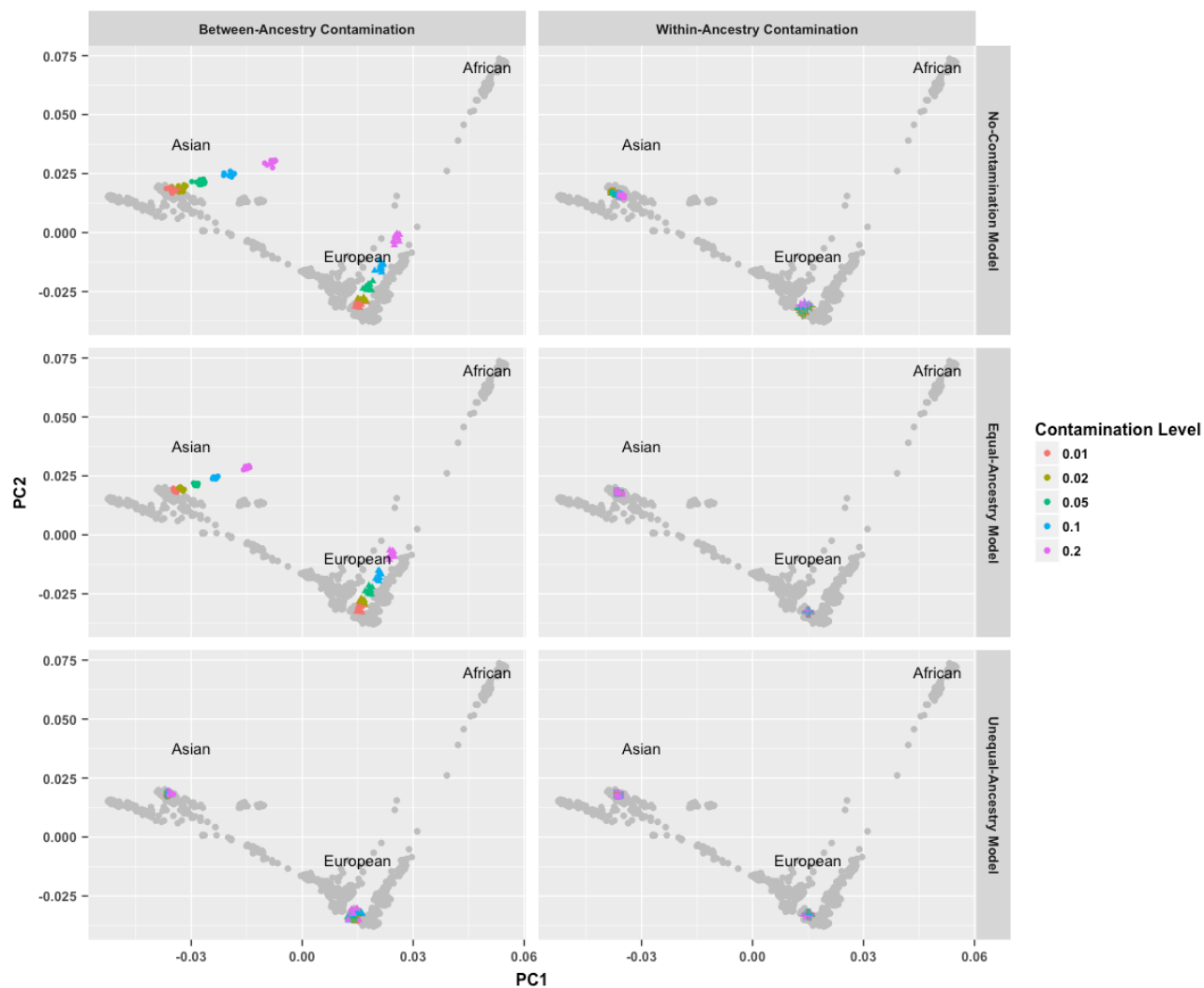
462 Comparison of contamination estimation between using *verifyBamID* and *verifyBamID2* on 500
463 InPSYght samples. All subjects are African Americans. Each dot represents the pair of contamination
464 rate estimates using different methods. The left panel shows the estimated contamination rates of
465 the original *verifyBamID* with pooled allele frequencies, which is the default setting of *verifyBamID* in
466 x-axis. Y-axis shows *verifyBamID2* with unequal-ancestry model (y-axis). Each point represents a
467 sequenced subject. The right panel compares the estimated contamination rates between two
468 models (unequal-ancestry vs. equal-ancestry) of *verifyBamID2* on the same dataset.

469



470 Figure 1.

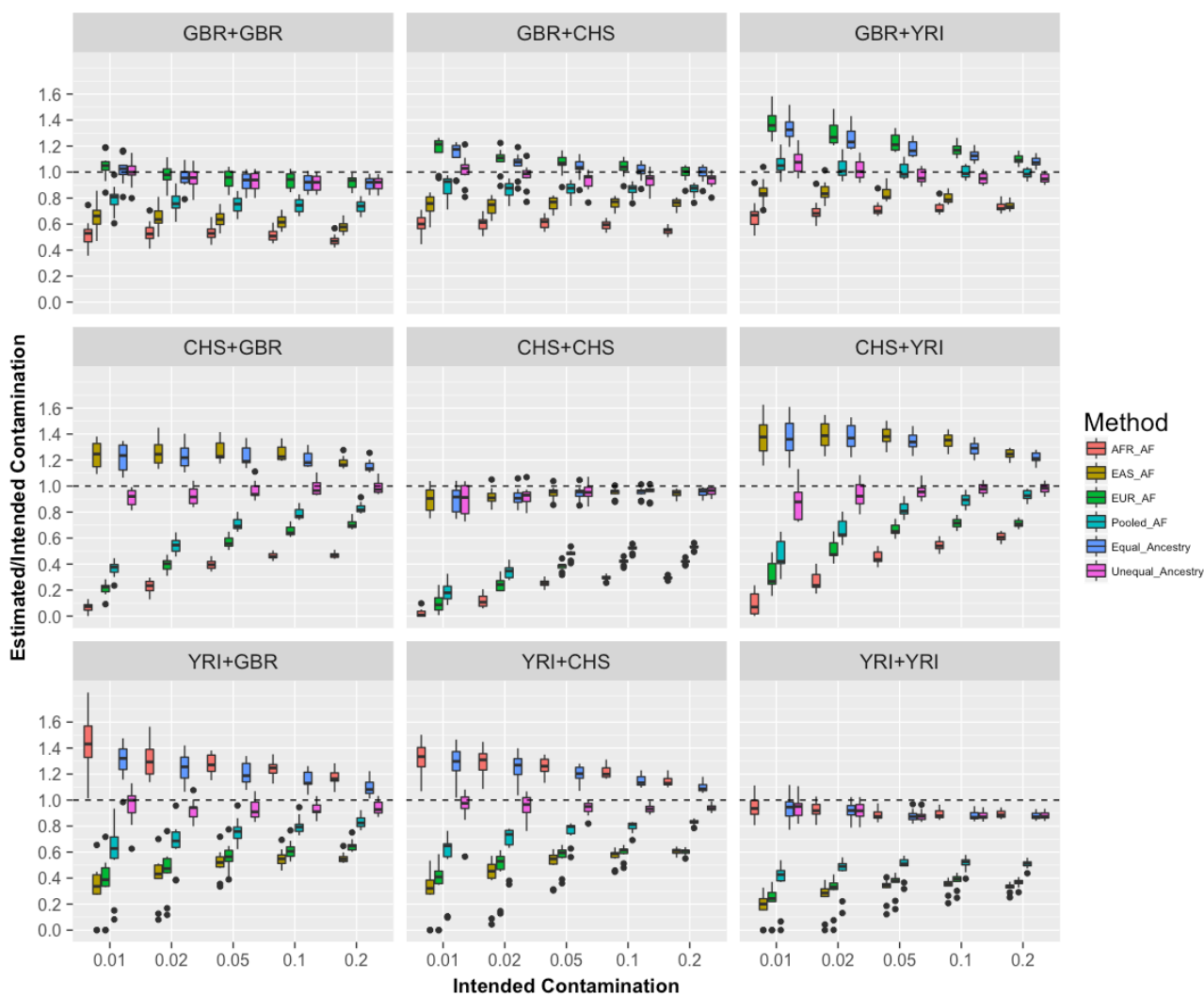
471 Evaluation of estimated genetic ancestry coordinates, in the absence of contamination, between
 472 *TRACE*, *LASER*, and *verifyBamID2* on samples from the 1000 Genomes low coverage genome (n=500,
 473 diverse ancestry) sequence data (A,C,E) and from the InPSYght deep genome (n=500, African
 474 Americans) sequence data (B,D,F). Panel A and B show results from *TRACE*, C and D from *LASER*, and
 475 E and F from *verifyBamID2* (assuming no contamination). Each point represents a sample, each color
 476 represents a population ancestry with the exception that grey point represents PCA coordinates of
 477 reference (HGDP) samples.
 478



479

480 Figure 2.

481 Impact of DNA sample contamination on the estimation of genetic ancestry. Each point represents a
482 sample. Grey point represents reference (HGDP) sample and its PCA coordinates, similar to Figure 1.
483 Each colored point represents *in-silico* contaminated samples across various contamination rates and
484 populations. In panel A, C, E, European (GBR) and East Asian (CHS) samples are contaminated with
485 African (YRI) samples at different contamination rates (i.e. between-ancestry contamination). In
486 panel B, D, F, European (GBR) and East Asian (CHS) samples are contamination with another sample
487 in the same population (i.e. within-ancestry contamination). Different colors represent different
488 contamination rate ranging from 1% to 20%. Upper panels (A, B) show *verifyBamID2* estimates
489 without modelling contamination. Middle panels (C, D) show *verifyBamID2* estimates under the
490 assumption that intended and contaminating populations are identical (i.e. equal-ancestry model).
491 Lower panels (E, F) show *verifyBamID2* estimates under the assumption that intended and
492 contaminating populations can be different (i.e. unequal-ancestry model).
493



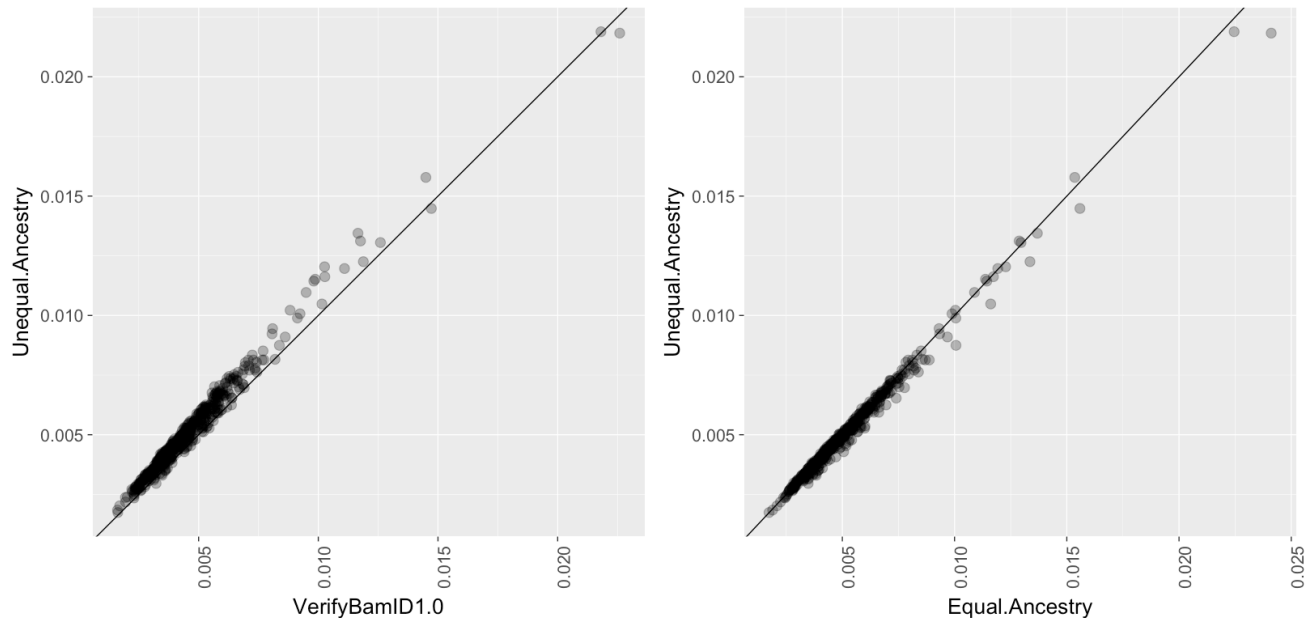
494

495

496 Figure 3.

497 Comparison of different models to estimate contamination rates. Horizontal (x) axis shows intended
 498 Contamination rate, vertical (y) axis shows the ratio of estimated to intended contamination rates.
 499 Each color represents different models to estimate contamination rates. EUR_AF, EAS_AF, AFR_AF
 500 represents old *verifyBamID* using European, East Asian, and African allele frequencies across the
 501 continental population using the 1000 Genomes data. Pooled_AF represents the old *verifyBamID*
 502 using aggregated allele frequencies across all 2,504 individuals in the 1000 Genomes Project.
 503 “Equal_Ancestry” represents the *verifyBamID2* assuming that intended and contaminating samples
 504 belong to the same population. “Unequal_Ancestry” represents *verifyBamID2* allowing different
 505 genetic ancestries between intended and contaminating samples (recommended setting). Each panel
 506 represents different combinations of intended (row) and contaminating (column) populations, in the
 507 order of GBR, CHS, and YRI.

508



509

510 Figure 4.
511 Comparison of contamination estimation between using *verifyBamID* and *verifyBamID2* on 500
512 InPSYght samples. All subjects are African Americans. Each dot represents the pair of contamination
513 rate estimates using different methods. The left panel shows the estimated contamination rates of
514 the original *verifyBamID* with pooled allele frequencies, which is the default setting of *verifyBamID*
515 in x-axis. Y-axis shows *verifyBamID2* with unequal-ancestry model (y-axis). Each point represents a
516 sequenced subject. The right panel compares the estimated contamination rates between two
517 models (unequal-ancestry vs. equal-ancestry) of *verifyBamID2* on the same dataset.

518 **Supplementary Materials**

519 **Supplementary Table S1:** Mean estimated contamination rates of *in-silico* contaminated population
 520 across different intended contamination rate, populations of intended and contaminating samples,
 521 and the estimation methods.
 522

Population		Intended % Contam.	Equal-Ancestry (VB2)	Unequal-Ancestry (VB2)	Pooled AF (VB1)	EUR AF (VB1)	EAS AF (VB1)	AFR AF (VB1)
Intended	Contam.							
GBR	GBR	1%	1.0%	1.0%	0.8%	1.0%	0.6%	0.5%
		2%	1.9%	1.9%	1.5%	2.0%	1.3%	1.1%
		5%	4.6%	4.6%	3.8%	4.7%	3.2%	2.7%
		10%	9.2%	9.2%	7.4%	9.4%	6.2%	5.2%
		20%	18.3%	18.3%	14.7%	18.5%	11.6%	9.5%
GBR	CHS	1%	1.1%	1.0%	0.9%	1.2%	0.7%	0.6%
		2%	2.1%	1.9%	1.7%	2.2%	1.5%	1.2%
		5%	5.2%	4.7%	4.3%	5.3%	3.8%	3.1%
		10%	10.1%	9.4%	8.6%	10.4%	7.6%	5.9%
		20%	19.8%	18.7%	17.3%	19.9%	15.1%	10.9%
GBR	YRI	1%	1.3%	1.1%	1.1%	1.4%	0.8%	0.7%
		2%	2.5%	2.0%	2.1%	2.6%	1.7%	1.4%
		5%	5.9%	4.8%	5.0%	6.1%	4.2%	3.6%
		10%	11.3%	9.5%	10.0%	11.7%	8.0%	7.3%
		20%	21.6%	19.1%	19.7%	22.0%	14.8%	14.6%
CHS	GBR	1%	1.2%	0.9%	0.4%	0.2%	1.2%	0.1%
		2%	2.5%	1.8%	1.1%	0.8%	2.5%	0.5%
		5%	6.1%	4.8%	3.6%	2.9%	6.3%	2.0%
		10%	12.0%	9.9%	7.9%	6.6%	12.5%	4.6%
		20%	23.0%	19.8%	16.6%	14.2%	23.6%	9.4%
CHS	CHS	1%	0.9%	0.9%	0.2%	0.1%	0.9%	0.0%
		2%	1.8%	1.8%	0.7%	0.5%	1.8%	0.2%
		5%	4.7%	4.8%	2.4%	1.9%	4.7%	1.3%
		10%	9.5%	9.5%	5.2%	4.2%	9.5%	2.9%
		20%	19.1%	19.1%	10.6%	8.4%	18.9%	5.9%
CHS	YRI	1%	1.4%	0.9%	0.5%	0.3%	1.4%	0.1%
		2%	2.8%	1.9%	1.3%	1.0%	2.8%	0.5%
		5%	6.7%	4.8%	4.1%	3.3%	6.9%	2.3%
		10%	12.9%	9.8%	8.9%	7.2%	13.5%	5.4%
		20%	24.3%	19.6%	18.6%	14.2%	24.9%	12.2%
YRI	GBR	1%	1.3%	1.0%	0.6%	0.4%	0.4%	1.4%

		2%	2.5%	1.9%	1.3%	0.9%	0.8%	2.6%
		5%	6.0%	4.6%	3.8%	2.8%	2.6%	6.4%
		10%	11.5%	9.3%	8.1%	6.2%	5.6%	12.5%
		20%	21.9%	18.8%	16.7%	13.0%	11.1%	23.5%
YRI	CHS	1%	1.3%	0.9%	0.5%	0.4%	0.3%	1.3%
		2%	2.5%	1.9%	1.3%	0.9%	0.8%	2.6%
		5%	6.0%	4.7%	3.8%	2.8%	2.5%	6.3%
		10%	11.5%	9.3%	7.9%	5.9%	5.6%	12.2%
		20%	22.0%	18.8%	16.6%	12.0%	12.1%	22.9%
YRI	YRI	1%	0.9%	0.9%	0.4%	0.2%	0.2%	0.9%
		2%	1.8%	1.8%	0.9%	0.6%	0.5%	1.8%
		5%	4.4%	4.4%	2.4%	1.8%	1.6%	4.4%
		10%	8.8%	8.8%	5.1%	3.8%	3.4%	8.9%
		20%	17.6%	17.6%	10.1%	7.3%	6.6%	17.9%

523

Equal-Ancestry Model: Estimate from *verifyBamID2* assuming intended and contaminating samples have the same genetic ancestry (in PC coordinates)

Unequal-Ancestry Model: Estimate from *verifyBamID2* allowing intended and contaminating samples to have different genetic ancestry

Pooled AF: Estimate from original *verifyBamID* using allele frequency across all 1000 Genomes phase 3 samples

EUR AF: Estimate from original *verifyBamID* using allele frequency across European subset of 1000 Genomes phase 3 samples

EAS AF: Estimate from original *verifyBamID* using allele frequency across East Asian subset of 1000 Genomes phase 3 samples

AFR AF: Estimate from original *verifyBamID* using allele frequency across African subset of 1000 Genomes phase 3 samples

524

Supplementary Table S2: Average of estimated contamination rates across 10 *in-silico* contaminated samples from Mexican population under different models. Results are similar as Europeans, except that unequal-ancestry model slightly reduces estimated contamination rate from equal-ancestry model, unlike GBR.

Intended % Contamination	Equal-Ancestry (VB2)	Unequal-Ancestry (VB2)	Pooled AF (VB1)	EUR AF (VB1)	EAS AF (VB1)	AFR AF (VB1)
1%	1.1%	1.0%	0.8%	1.0%	0.6%	0.3%
2%	2.1%	2.1%	1.6%	2.0%	1.4%	0.9%
5%	4.8%	4.8%	3.9%	4.6%	3.5%	2.5%
10%	9.3%	9.2%	7.8%	8.8%	6.8%	4.9%
20%	18.5%	18.3%	15.4%	17.0%	13.0%	9.4%

525

Supplementary Table S3: Comparison of mean contamination rate ratio (Estimated/Intended) using different size of marker set (under Unequal-Ancestry Model). The Numbers in parenthesis represent standard deviation.

Sample Population		Marker Set	Intended Contamination Rate				
Intended	Contam.		0.01	0.02	0.05	0.1	0.2
GBR	GBR	1K	0.57(0.15)	0.88(0.38)	0.87(0.28)	0.92(0.18)	0.95(0.12)
		10K	0.98(0.13)	0.95(0.11)	0.93(0.09)	0.91(0.08)	0.91(0.07)
		100K	1.00(0.10)	0.96(0.09)	0.93(0.08)	0.92(0.06)	0.91(0.05)
CHS	CHS	1K	1.38(1.26)	1.09(0.63)	1.00(0.44)	0.95(0.41)	0.95(0.21)
		10K	1.08(0.48)	1.03(0.26)	1.00(0.12)	1.01(0.08)	0.96(0.06)
		100K	0.89(0.12)	0.92(0.08)	0.95(0.07)	0.95(0.05)	0.96(0.04)
YRI	YRI	1K	1.23(0.86)	0.92(0.46)	0.98(0.30)	0.95(0.16)	0.97(0.10)
		10K	0.91(0.20)	0.87(0.17)	0.89(0.05)	0.88(0.04)	0.90(0.03)
		100K	0.94(0.08)	0.92(0.07)	0.88(0.04)	0.88(0.04)	0.88(0.03)
CHS	YRI	1K	1.07(0.90)	1.03(0.61)	0.95(0.37)	0.97(0.22)	0.91(0.12)
		10K	1.00(0.46)	0.99(0.22)	1.02(0.12)	1.02(0.08)	0.99(0.06)
		100K	0.88(0.14)	0.93(0.10)	0.96(0.06)	0.98(0.05)	0.98(0.04)
YRI	CHS	1K	1.00(0.49)	1.00(0.35)	0.91(0.24)	1.00(0.17)	1.01(0.10)
		10K	1.02(0.10)	1.00(0.07)	0.95(0.03)	0.94(0.03)	0.94(0.02)
		100K	0.94(0.15)	0.95(0.09)	0.93(0.05)	0.93(0.03)	0.94(0.03)
GBR	YRI	1K	1.10(0.49)	1.10(0.28)	1.06(0.30)	0.98(0.18)	0.97(0.09)
		10K	0.94(0.23)	0.98(0.10)	0.94(0.06)	0.93(0.04)	0.94(0.03)
		100K	1.07(0.09)	1.02(0.08)	0.97(0.06)	0.95(0.05)	0.95(0.04)
YRI	GBR	1K	1.13(0.56)	0.78(0.36)	0.84(0.19)	0.93(0.11)	0.98(0.06)
		10K	0.92(0.24)	0.89(0.15)	0.91(0.06)	0.93(0.05)	0.94(0.05)
		100K	0.95(0.15)	0.93(0.08)	0.93(0.08)	0.93(0.06)	0.94(0.06)
CHS	GBR	1K	1.28(1.24)	1.12(0.70)	1.00(0.40)	0.95(0.21)	0.97(0.13)
		10K	1.06(0.54)	1.01(0.33)	1.00(0.14)	1.00(0.07)	0.98(0.05)
		100K	0.91(0.06)	0.92(0.07)	0.97(0.07)	0.99(0.06)	0.99(0.05)
GBR	CHS	1K	0.89(0.47)	0.83(0.42)	0.84(0.17)	0.91(0.14)	0.92(0.13)
		10K	0.97(0.17)	0.93(0.11)	0.94(0.08)	0.94(0.06)	0.92(0.06)
		100K	1.01(0.12)	0.97(0.10)	0.93(0.08)	0.94(0.07)	0.94(0.06)

527 **Supplementary Table S4.** A full table summarizing the contamination rate ratio (Estimated/Intended) across vari-
 528 ous simulation parameters, populations, and estimation methods shown in Figure 3. 100K marker sets were used.

Sample Population		Method	Allele Frequencies	Intended % Contam	Mean	SD	MSE
In-tended	Contam.						
GBR	GBR	VB1	AFR	1%	0.52	0.11	0.242
GBR	GBR	VB1	AFR	2%	0.53	0.09	0.223
GBR	GBR	VB1	AFR	5%	0.53	0.06	0.221
GBR	GBR	VB1	AFR	10%	0.52	0.05	0.237
GBR	GBR	VB1	AFR	20%	0.48	0.04	0.276
GBR	GBR	VB1	EUR	1%	1.04	0.10	0.012
GBR	GBR	VB1	EUR	2%	0.98	0.09	0.007
GBR	GBR	VB1	EUR	5%	0.95	0.07	0.008
GBR	GBR	VB1	EUR	10%	0.94	0.06	0.008
GBR	GBR	VB1	EUR	20%	0.92	0.05	0.008
GBR	GBR	VB1	EAS	1%	0.65	0.11	0.136
GBR	GBR	VB1	EAS	2%	0.65	0.09	0.132
GBR	GBR	VB1	EAS	5%	0.64	0.06	0.135
GBR	GBR	VB1	EAS	10%	0.62	0.05	0.148
GBR	GBR	VB1	EAS	20%	0.58	0.05	0.179
GBR	GBR	VB1	Pooled	1%	0.79	0.11	0.055
GBR	GBR	VB1	Pooled	2%	0.77	0.08	0.060
GBR	GBR	VB1	Pooled	5%	0.75	0.07	0.066
GBR	GBR	VB1	Pooled	10%	0.74	0.06	0.069
GBR	GBR	VB1	Pooled	20%	0.73	0.05	0.073
GBR	GBR	VB2	ISAF (Equal-Ancestry)	1%	1.02	0.11	0.010
GBR	GBR	VB2	ISAF (Equal-Ancestry)	2%	0.96	0.09	0.009
GBR	GBR	VB2	ISAF (Equal -Ancestry)	5%	0.93	0.07	0.010
GBR	GBR	VB2	ISAF (Equal -Ancestry)	10%	0.92	0.06	0.010
GBR	GBR	VB2	ISAF (Equal -Ancestry)	20%	0.91	0.05	0.010
GBR	GBR	VB2	ISAF (Unequal-Ancestry)	1%	1.00	0.10	0.009
GBR	GBR	VB2	ISAF (Unequal-Ancestry)	2%	0.96	0.09	0.009
GBR	GBR	VB2	ISAF (Unequal-Ancestry)	5%	0.93	0.08	0.011
GBR	GBR	VB2	ISAF (Unequal-Ancestry)	10%	0.92	0.06	0.010
GBR	GBR	VB2	ISAF (Unequal-Ancestry)	20%	0.91	0.05	0.010
GBR	CHS	VB1	AFR	1%	0.59	0.08	0.172
GBR	CHS	VB1	AFR	2%	0.60	0.06	0.162
GBR	CHS	VB1	AFR	5%	0.61	0.05	0.154
GBR	CHS	VB1	AFR	10%	0.59	0.04	0.169
GBR	CHS	VB1	AFR	20%	0.55	0.03	0.206

GBR	CHS	VB1	EUR	1%	1.17	0.11	0.039
GBR	CHS	VB1	EUR	2%	1.09	0.10	0.016
GBR	CHS	VB1	EUR	5%	1.06	0.08	0.010
GBR	CHS	VB1	EUR	10%	1.04	0.07	0.006
GBR	CHS	VB1	EUR	20%	0.99	0.06	0.003
GBR	CHS	VB1	EAS	1%	0.74	0.09	0.074
GBR	CHS	VB1	EAS	2%	0.74	0.07	0.072
GBR	CHS	VB1	EAS	5%	0.76	0.06	0.063
GBR	CHS	VB1	EAS	10%	0.76	0.05	0.061
GBR	CHS	VB1	EAS	20%	0.75	0.04	0.062
GBR	CHS	VB1	Pooled	1%	0.89	0.09	0.019
GBR	CHS	VB1	Pooled	2%	0.86	0.07	0.025
GBR	CHS	VB1	Pooled	5%	0.86	0.06	0.022
GBR	CHS	VB1	Pooled	10%	0.86	0.06	0.022
GBR	CHS	VB1	Pooled	20%	0.86	0.05	0.021
GBR	CHS	VB2	ISAF (Equal-Ancestry)	1%	1.13	0.11	0.028
GBR	CHS	VB2	ISAF (Equal-Ancestry)	2%	1.06	0.09	0.011
GBR	CHS	VB2	ISAF (Equal -Ancestry)	5%	1.03	0.08	0.007
GBR	CHS	VB2	ISAF (Equal -Ancestry)	10%	1.01	0.07	0.004
GBR	CHS	VB2	ISAF (Equal -Ancestry)	20%	0.99	0.06	0.004
GBR	CHS	VB2	ISAF (Unequal-Ancestry)	1%	1.01	0.12	0.012
GBR	CHS	VB2	ISAF (Unequal-Ancestry)	2%	0.97	0.10	0.010
GBR	CHS	VB2	ISAF (Unequal-Ancestry)	5%	0.93	0.08	0.010
GBR	CHS	VB2	ISAF (Unequal-Ancestry)	10%	0.94	0.07	0.008
GBR	CHS	VB2	ISAF (Unequal-Ancestry)	20%	0.94	0.06	0.007
GBR	YRI	VB1	AFR	1%	0.67	0.11	0.119
GBR	YRI	VB1	AFR	2%	0.70	0.09	0.096
GBR	YRI	VB1	AFR	5%	0.72	0.06	0.082
GBR	YRI	VB1	AFR	10%	0.73	0.05	0.077
GBR	YRI	VB1	AFR	20%	0.73	0.04	0.074
GBR	YRI	VB1	EUR	1%	1.38	0.10	0.150
GBR	YRI	VB1	EUR	2%	1.30	0.09	0.097
GBR	YRI	VB1	EUR	5%	1.23	0.07	0.055
GBR	YRI	VB1	EUR	10%	1.17	0.05	0.032
GBR	YRI	VB1	EUR	20%	1.10	0.04	0.011
GBR	YRI	VB1	EAS	1%	0.85	0.10	0.032
GBR	YRI	VB1	EAS	2%	0.85	0.08	0.028
GBR	YRI	VB1	EAS	5%	0.83	0.06	0.031
GBR	YRI	VB1	EAS	10%	0.80	0.04	0.042
GBR	YRI	VB1	EAS	20%	0.74	0.03	0.069

GBR	YRI	VB1	Pooled	1%	1.05	0.09	0.010
GBR	YRI	VB1	Pooled	2%	1.03	0.08	0.007
GBR	YRI	VB1	Pooled	5%	1.01	0.06	0.003
GBR	YRI	VB1	Pooled	10%	1.00	0.05	0.002
GBR	YRI	VB1	Pooled	20%	0.99	0.04	0.002
GBR	YRI	VB2	ISAF (Equal-Ancestry)	1%	1.33	0.09	0.118
GBR	YRI	VB2	ISAF (Equal-Ancestry)	2%	1.26	0.09	0.074
GBR	YRI	VB2	ISAF (Equal -Ancestry)	5%	1.18	0.06	0.036
GBR	YRI	VB2	ISAF (Equal -Ancestry)	10%	1.13	0.05	0.018
GBR	YRI	VB2	ISAF (Equal -Ancestry)	20%	1.08	0.04	0.008
GBR	YRI	VB2	ISAF (Unequal-Ancestry)	1%	1.07	0.09	0.014
GBR	YRI	VB2	ISAF (Unequal-Ancestry)	2%	1.02	0.08	0.006
GBR	YRI	VB2	ISAF (Unequal-Ancestry)	5%	0.97	0.06	0.004
GBR	YRI	VB2	ISAF (Unequal-Ancestry)	10%	0.95	0.05	0.004
GBR	YRI	VB2	ISAF (Unequal-Ancestry)	20%	0.95	0.04	0.004
CHS	GBR	VB1	AFR	1%	0.07	0.04	0.868
CHS	GBR	VB1	AFR	2%	0.23	0.05	0.597
CHS	GBR	VB1	AFR	5%	0.40	0.04	0.366
CHS	GBR	VB1	AFR	10%	0.46	0.03	0.290
CHS	GBR	VB1	AFR	20%	0.47	0.02	0.282
CHS	GBR	VB1	EUR	1%	0.21	0.05	0.625
CHS	GBR	VB1	EUR	2%	0.40	0.05	0.364
CHS	GBR	VB1	EUR	5%	0.57	0.05	0.184
CHS	GBR	VB1	EUR	10%	0.66	0.04	0.119
CHS	GBR	VB1	EUR	20%	0.71	0.04	0.087
CHS	GBR	VB1	EAS	1%	1.24	0.11	0.069
CHS	GBR	VB1	EAS	2%	1.26	0.10	0.075
CHS	GBR	VB1	EAS	5%	1.27	0.08	0.077
CHS	GBR	VB1	EAS	10%	1.25	0.06	0.066
CHS	GBR	VB1	EAS	20%	1.18	0.05	0.035
CHS	GBR	VB1	Pooled	1%	0.36	0.06	0.409
CHS	GBR	VB1	Pooled	2%	0.55	0.06	0.207
CHS	GBR	VB1	Pooled	5%	0.71	0.05	0.086
CHS	GBR	VB1	Pooled	10%	0.79	0.05	0.047
CHS	GBR	VB1	Pooled	20%	0.83	0.04	0.031
CHS	GBR	VB2	ISAF (Equal-Ancestry)	1%	1.22	0.11	0.060
CHS	GBR	VB2	ISAF (Equal-Ancestry)	2%	1.23	0.10	0.060
CHS	GBR	VB2	ISAF (Equal -Ancestry)	5%	1.23	0.08	0.057
CHS	GBR	VB2	ISAF (Equal -Ancestry)	10%	1.20	0.06	0.044
CHS	GBR	VB2	ISAF (Equal -Ancestry)	20%	1.15	0.05	0.025

CHS	GBR	VB2	ISAF (Unequal-Ancestry)	1%	0.91	0.06	0.011
CHS	GBR	VB2	ISAF (Unequal-Ancestry)	2%	0.92	0.07	0.010
CHS	GBR	VB2	ISAF (Unequal-Ancestry)	5%	0.97	0.07	0.005
CHS	GBR	VB2	ISAF (Unequal-Ancestry)	10%	0.99	0.06	0.004
CHS	GBR	VB2	ISAF (Unequal-Ancestry)	20%	0.99	0.05	0.003
CHS	CHS	VB1	AFR	1%	0.02	0.03	0.956
CHS	CHS	VB1	AFR	2%	0.12	0.05	0.782
CHS	CHS	VB1	AFR	5%	0.25	0.03	0.562
CHS	CHS	VB1	AFR	10%	0.29	0.02	0.500
CHS	CHS	VB1	AFR	20%	0.29	0.01	0.500
CHS	CHS	VB1	EUR	1%	0.10	0.07	0.815
CHS	CHS	VB1	EUR	2%	0.24	0.05	0.573
CHS	CHS	VB1	EUR	5%	0.38	0.03	0.385
CHS	CHS	VB1	EUR	10%	0.42	0.02	0.338
CHS	CHS	VB1	EUR	20%	0.42	0.02	0.337
CHS	CHS	VB1	EAS	1%	0.90	0.10	0.020
CHS	CHS	VB1	EAS	2%	0.92	0.07	0.011
CHS	CHS	VB1	EAS	5%	0.95	0.06	0.006
CHS	CHS	VB1	EAS	10%	0.95	0.04	0.004
CHS	CHS	VB1	EAS	20%	0.94	0.03	0.004
CHS	CHS	VB1	Pooled	1%	0.19	0.08	0.659
CHS	CHS	VB1	Pooled	2%	0.34	0.05	0.435
CHS	CHS	VB1	Pooled	5%	0.48	0.04	0.275
CHS	CHS	VB1	Pooled	10%	0.52	0.03	0.233
CHS	CHS	VB1	Pooled	20%	0.53	0.02	0.222
CHS	CHS	VB2	ISAF (Equal-Ancestry)	1%	0.90	0.11	0.021
CHS	CHS	VB2	ISAF (Equal-Ancestry)	2%	0.91	0.07	0.012
CHS	CHS	VB2	ISAF (Equal -Ancestry)	5%	0.95	0.06	0.006
CHS	CHS	VB2	ISAF (Equal -Ancestry)	10%	0.95	0.04	0.004
CHS	CHS	VB2	ISAF (Equal -Ancestry)	20%	0.95	0.03	0.003
CHS	CHS	VB2	ISAF (Unequal-Ancestry)	1%	0.89	0.12	0.024
CHS	CHS	VB2	ISAF (Unequal-Ancestry)	2%	0.92	0.08	0.012
CHS	CHS	VB2	ISAF (Unequal-Ancestry)	5%	0.95	0.07	0.006
CHS	CHS	VB2	ISAF (Unequal-Ancestry)	10%	0.95	0.05	0.004
CHS	CHS	VB2	ISAF (Unequal-Ancestry)	20%	0.96	0.04	0.003
CHS	YRI	VB1	AFR	1%	0.09	0.09	0.828
CHS	YRI	VB1	AFR	2%	0.27	0.08	0.543
CHS	YRI	VB1	AFR	5%	0.45	0.05	0.302
CHS	YRI	VB1	AFR	10%	0.54	0.04	0.210
CHS	YRI	VB1	AFR	20%	0.61	0.03	0.155

CHS	YRI	VB1	EUR	1%	0.31	0.11	0.492
CHS	YRI	VB1	EUR	2%	0.51	0.08	0.250
CHS	YRI	VB1	EUR	5%	0.67	0.05	0.114
CHS	YRI	VB1	EUR	10%	0.72	0.04	0.083
CHS	YRI	VB1	EUR	20%	0.71	0.03	0.084
CHS	YRI	VB1	EAS	1%	1.38	0.14	0.161
CHS	YRI	VB1	EAS	2%	1.39	0.10	0.163
CHS	YRI	VB1	EAS	5%	1.38	0.07	0.151
CHS	YRI	VB1	EAS	10%	1.35	0.06	0.123
CHS	YRI	VB1	EAS	20%	1.24	0.04	0.061
CHS	YRI	VB1	Pooled	1%	0.47	0.13	0.298
CHS	YRI	VB1	Pooled	2%	0.66	0.09	0.123
CHS	YRI	VB1	Pooled	5%	0.82	0.06	0.036
CHS	YRI	VB1	Pooled	10%	0.89	0.05	0.015
CHS	YRI	VB1	Pooled	20%	0.93	0.04	0.007
CHS	YRI	VB2	ISAF (Equal-Ancestry)	1%	1.37	0.14	0.157
CHS	YRI	VB2	ISAF (Equal-Ancestry)	2%	1.38	0.11	0.154
CHS	YRI	VB2	ISAF (Equal -Ancestry)	5%	1.34	0.07	0.122
CHS	YRI	VB2	ISAF (Equal -Ancestry)	10%	1.29	0.06	0.085
CHS	YRI	VB2	ISAF (Equal -Ancestry)	20%	1.22	0.05	0.048
CHS	YRI	VB2	ISAF (Unequal-Ancestry)	1%	0.88	0.14	0.033
CHS	YRI	VB2	ISAF (Unequal-Ancestry)	2%	0.93	0.10	0.014
CHS	YRI	VB2	ISAF (Unequal-Ancestry)	5%	0.96	0.06	0.005
CHS	YRI	VB2	ISAF (Unequal-Ancestry)	10%	0.98	0.05	0.002
CHS	YRI	VB2	ISAF (Unequal-Ancestry)	20%	0.98	0.04	0.002
YRI	GBR	VB1	AFR	1%	1.43	0.23	0.236
YRI	GBR	VB1	AFR	2%	1.31	0.14	0.113
YRI	GBR	VB1	AFR	5%	1.28	0.08	0.081
YRI	GBR	VB1	AFR	10%	1.25	0.07	0.065
YRI	GBR	VB1	AFR	20%	1.17	0.06	0.034
YRI	GBR	VB1	EUR	1%	0.36	0.22	0.453
YRI	GBR	VB1	EUR	2%	0.46	0.19	0.329
YRI	GBR	VB1	EUR	5%	0.56	0.11	0.201
YRI	GBR	VB1	EUR	10%	0.62	0.07	0.153
YRI	GBR	VB1	EUR	20%	0.65	0.05	0.124
YRI	GBR	VB1	EAS	1%	0.32	0.20	0.504
YRI	GBR	VB1	EAS	2%	0.41	0.18	0.380
YRI	GBR	VB1	EAS	5%	0.52	0.11	0.245
YRI	GBR	VB1	EAS	10%	0.55	0.07	0.204
YRI	GBR	VB1	EAS	20%	0.56	0.04	0.198

YRI	GBR	VB1	Pooled	1%	0.57	0.26	0.248
YRI	GBR	VB1	Pooled	2%	0.67	0.17	0.138
YRI	GBR	VB1	Pooled	5%	0.76	0.10	0.066
YRI	GBR	VB1	Pooled	10%	0.80	0.07	0.043
YRI	GBR	VB1	Pooled	20%	0.83	0.05	0.030
YRI	GBR	VB2	ISAF (Equal-Ancestry)	1%	1.30	0.15	0.107
YRI	GBR	VB2	ISAF (Equal-Ancestry)	2%	1.25	0.11	0.072
YRI	GBR	VB2	ISAF (Equal -Ancestry)	5%	1.20	0.09	0.048
YRI	GBR	VB2	ISAF (Equal -Ancestry)	10%	1.15	0.07	0.028
YRI	GBR	VB2	ISAF (Equal -Ancestry)	20%	1.10	0.07	0.013
YRI	GBR	VB2	ISAF (Unequal-Ancestry)	1%	0.95	0.15	0.021
YRI	GBR	VB2	ISAF (Unequal-Ancestry)	2%	0.93	0.08	0.012
YRI	GBR	VB2	ISAF (Unequal-Ancestry)	5%	0.93	0.08	0.011
YRI	GBR	VB2	ISAF (Unequal-Ancestry)	10%	0.93	0.06	0.008
YRI	GBR	VB2	ISAF (Unequal-Ancestry)	20%	0.94	0.06	0.006
YRI	CHS	VB1	AFR	1%	1.32	0.13	0.120
YRI	CHS	VB1	AFR	2%	1.30	0.11	0.098
YRI	CHS	VB1	AFR	5%	1.26	0.07	0.071
YRI	CHS	VB1	AFR	10%	1.22	0.05	0.049
YRI	CHS	VB1	AFR	20%	1.14	0.04	0.022
YRI	CHS	VB1	EUR	1%	0.35	0.20	0.455
YRI	CHS	VB1	EUR	2%	0.46	0.18	0.319
YRI	CHS	VB1	EUR	5%	0.56	0.10	0.204
YRI	CHS	VB1	EUR	10%	0.59	0.06	0.168
YRI	CHS	VB1	EUR	20%	0.60	0.03	0.159
YRI	CHS	VB1	EAS	1%	0.29	0.17	0.528
YRI	CHS	VB1	EAS	2%	0.40	0.18	0.395
YRI	CHS	VB1	EAS	5%	0.51	0.11	0.252
YRI	CHS	VB1	EAS	10%	0.56	0.06	0.194
YRI	CHS	VB1	EAS	20%	0.61	0.03	0.157
YRI	CHS	VB1	Pooled	1%	0.55	0.24	0.259
YRI	CHS	VB1	Pooled	2%	0.66	0.16	0.136
YRI	CHS	VB1	Pooled	5%	0.75	0.09	0.068
YRI	CHS	VB1	Pooled	10%	0.79	0.04	0.044
YRI	CHS	VB1	Pooled	20%	0.83	0.02	0.030
YRI	CHS	VB2	ISAF (Equal-Ancestry)	1%	1.29	0.13	0.098
YRI	CHS	VB2	ISAF (Equal-Ancestry)	2%	1.25	0.11	0.074
YRI	CHS	VB2	ISAF (Equal -Ancestry)	5%	1.20	0.07	0.043
YRI	CHS	VB2	ISAF (Equal -Ancestry)	10%	1.15	0.04	0.023
YRI	CHS	VB2	ISAF (Equal -Ancestry)	20%	1.10	0.04	0.011

YRI	CHS	VB2	ISAF (Unequal-Ancestry)	1%	0.94	0.15	0.023
YRI	CHS	VB2	ISAF (Unequal-Ancestry)	2%	0.95	0.09	0.010
YRI	CHS	VB2	ISAF (Unequal-Ancestry)	5%	0.93	0.05	0.007
YRI	CHS	VB2	ISAF (Unequal-Ancestry)	10%	0.93	0.03	0.005
YRI	CHS	VB2	ISAF (Unequal-Ancestry)	20%	0.94	0.03	0.004
YRI	YRI	VB1	AFR	1%	0.95	0.09	0.010
YRI	YRI	VB1	AFR	2%	0.92	0.06	0.009
YRI	YRI	VB1	AFR	5%	0.89	0.05	0.014
YRI	YRI	VB1	AFR	10%	0.89	0.04	0.013
YRI	YRI	VB1	AFR	20%	0.89	0.03	0.012
YRI	YRI	VB1	EUR	1%	0.22	0.13	0.619
YRI	YRI	VB1	EUR	2%	0.29	0.14	0.518
YRI	YRI	VB1	EUR	5%	0.36	0.09	0.423
YRI	YRI	VB1	EUR	10%	0.38	0.06	0.391
YRI	YRI	VB1	EUR	20%	0.36	0.03	0.405
YRI	YRI	VB1	EAS	1%	0.18	0.11	0.680
YRI	YRI	VB1	EAS	2%	0.25	0.13	0.575
YRI	YRI	VB1	EAS	5%	0.32	0.09	0.474
YRI	YRI	VB1	EAS	10%	0.34	0.06	0.438
YRI	YRI	VB1	EAS	20%	0.33	0.03	0.452
YRI	YRI	VB1	Pooled	1%	0.36	0.18	0.433
YRI	YRI	VB1	Pooled	2%	0.44	0.14	0.333
YRI	YRI	VB1	Pooled	5%	0.49	0.08	0.267
YRI	YRI	VB1	Pooled	10%	0.51	0.05	0.242
YRI	YRI	VB1	Pooled	20%	0.51	0.03	0.245
YRI	YRI	VB2	ISAF (Equal-Ancestry)	1%	0.94	0.10	0.012
YRI	YRI	VB2	ISAF (Equal-Ancestry)	2%	0.92	0.06	0.011
YRI	YRI	VB2	ISAF (Equal -Ancestry)	5%	0.88	0.04	0.016
YRI	YRI	VB2	ISAF (Equal -Ancestry)	10%	0.88	0.04	0.015
YRI	YRI	VB2	ISAF (Equal -Ancestry)	20%	0.88	0.03	0.015
YRI	YRI	VB2	ISAF (Unequal-Ancestry)	1%	0.94	0.08	0.010
YRI	YRI	VB2	ISAF (Unequal-Ancestry)	2%	0.92	0.07	0.011
YRI	YRI	VB2	ISAF (Unequal-Ancestry)	5%	0.88	0.04	0.016
YRI	YRI	VB2	ISAF (Unequal-Ancestry)	10%	0.88	0.04	0.015
YRI	YRI	VB2	ISAF (Unequal-Ancestry)	20%	0.88	0.03	0.015